



## GALPROP Code for Galactic Cosmic Ray Propagation and Associated Photon Emissions

I. V. MOSKALENKO<sup>1,2</sup>, S. DIGEL<sup>2,3</sup>, G. JÓHANNESSON<sup>4</sup>, E. ORLANDO<sup>1</sup>, T. A. PORTER<sup>1</sup>, R. RUIZ DE AUSTRI<sup>5</sup>, A. W. STRONG<sup>6</sup>, R. TROTTA<sup>7</sup>, A. E. VLADIMIROV<sup>1</sup>

<sup>1</sup>*Hansen Experimental Physics Laboratory, Stanford University, Stanford, CA 94305, U.S.A.*

<sup>2</sup>*Kavli Institute for Particle Astrophysics and Cosmology, Stanford University, Stanford, CA 94305, U.S.A.*

<sup>3</sup>*SLAC National Accelerator Laboratory, 2575 Sand Hill Road, Menlo Park, CA 94025, U.S.A.*

<sup>4</sup>*Science Institute, University of Iceland, Dunhaga 5, IS-107 Reykjavik, Iceland*

<sup>5</sup>*Instituto de Física Corpuscular, IFIC-UV/CSIC, Valencia, Spain*

<sup>6</sup>*Max-Planck-Institut für extraterrestrische Physik, Postfach 1312, D-85741 Garching, Germany*

<sup>7</sup>*Astrophysics Group, Imperial College London, Blackett Laboratory, Prince Consort Road, London SW7 2AZ, UK*  
imos@stanford.edu

DOI: 10.7529/ICRC2011/V06/1194

**Abstract:** Research in many areas of modern physics such as, e.g., indirect searches for dark matter and particle acceleration in supernova remnant shocks rely heavily on studies of cosmic rays (CRs) and associated diffuse emissions (radio, microwave, X-rays,  $\gamma$ -rays). The numerical Galactic CR propagation code GALPROP has been shown to reproduce simultaneously observational data of many kinds related to CR origin and propagation. We report on the latest updates of GALPROP, development of WebRun, a service to the scientific community enabling easy use of the GALPROP code via web browsers, and a library of evaluated isotopic production cross sections. We also report the results of a full Bayesian analysis of propagation parameters using nested sampling and Markov Chain Monte Carlo methods (implemented in the SuperBayeS code).

**Keywords:** Galaxy, cosmic rays, elementary particles, diffuse radio emission, diffuse optical emission, diffuse X-rays, diffuse  $\gamma$ -rays, interstellar medium, propagation, fragmentation, energy losses, Bayesian analysis

### 1 The GALPROP code

The GALPROP project [1, 2] began in late 1996 and has now 15 years of development behind it<sup>1</sup>. The code, originally written in fortran90, was made public in 1998. A version rewritten in C++ was produced in 2001, and the most recent public version 54 was recently released [3]. The code is available from the dedicated website<sup>2</sup> where a facility for users to run the code via online forms in a web-browser is also provided. The key concept underlying the GALPROP code is that various kinds of data, e.g., direct CR measurements including primary and secondary nuclei, electrons and positrons,  $\gamma$ -rays, synchrotron radiation, and so forth, are all related to the same astrophysical components of the Galaxy and hence have to be modeled self-consistently [4]. The goal is for GALPROP-based models to be as realistic as possible and to make use of available astronomical information, nuclear and particle data, with a minimum of simplifying assumptions. A complete description of the rationale and motivation is given in the review [5]. A very short summary of GALPROP is provided below; for details the reader is referred to the relevant papers [1, 2, 3, 6, 7, 8, 9, 10, 11].

The GALPROP code solves the CR transport equation with a given source distribution and boundary conditions for all CR species [2]. This includes a galactic wind (convection), diffusive reacceleration in the ISM, energy losses, nuclear fragmentation, radioactive decay, and production of secondary particles and isotopes. The distribution of CR sources can be specified as required ([12] shows an example of the source distribution derived from the fit to the *Fermi*-LAT data). The numerical solution of the transport equation is based on a Crank-Nicholson implicit second-order scheme [13]. The spatial boundary conditions assume free particle escape. For a given halo size the diffusion coefficient, as a function of momentum and the reacceleration or convection parameters, is determined from secondary/primary ratios. If reacceleration is included, the momentum-space diffusion coefficient  $D_{pp}$  is related to the spatial coefficient  $D_{xx}$  ( $= \beta D_0 \rho^\delta$ ) [14], where  $\delta = 1/3$  for a Kolmogorov spectrum of interstellar turbulence or  $\delta = 1/2$  for a Kraichnan cascade (but can also be arbitrary),  $\rho \equiv pc/Ze$  is the magnetic rigidity. Non-linear wave damping [11] can also be included if required.

1. <http://sciencenewswatch.com/dr/erf/2009/09octerf/09octerfStronET/>  
2. <http://galprop.stanford.edu>

Cross-sections are based on the extensive LANL database, nuclear codes, and parameterizations [15]. The most important isotopic production cross-sections are calculated using our fits to major production channels [8, 16]. Other cross-sections are computed using phenomenological approximations [17] and/or [18] renormalized to the data where they exist. The nuclear reaction network is built using the Nuclear Data Sheets. A new project to improve on the calculations of the isotopic production cross sections (ISOPROCS project) is described in [19].

The GALPROP code computes a complete network of primary, secondary and tertiary CR production starting from input source abundances. Starting with the heaviest primary nucleus considered (e.g.  $^{64}\text{Ni}$ ) the propagation solution is used to compute the source term for its spallation products  $A - 1$ ,  $A - 2$  and so forth, which are then propagated in turn, and so on down to protons, secondary electrons and positrons, and antiprotons. To account for some special  $\beta^-$ -decay cases (e.g.,  $^{10}\text{Be} \rightarrow ^{10}\text{B}$ ) the whole loop is repeated twice. The inelastically scattered protons and antiprotons are treated as separate components (secondary protons, tertiary antiprotons). GALPROP includes K-capture and electron stripping processes as well as knock-on electrons.

Production of neutral pions, secondary positrons and electrons is calculated using the formalism [20, 21] as described in [1] with a correction from [22] or using a parameterization given in [23]. Antiproton production uses formalism described in [7].

The  $\gamma$ -ray and synchrotron emissivities are calculated using the propagated CR distributions, including a contribution from secondary particles such as positrons and electrons from inelastic processes in the ISM that increases the  $\gamma$ -ray flux at MeV energies [24, 25]. The inverse Compton (IC) scattering is treated using the appropriate formalism for an anisotropic radiation field [6] with the full spatial and angular distribution of the interstellar radiation field (ISRF) [26, 24]. Electron bremsstrahlung cross section is calculated as described in [9]. Intensity skymaps are then generated using the line of sight integration where the gas-related  $\gamma$ -ray intensities ( $\pi^0$ -decay, bremsstrahlung) are normalized to the column densities of H I and H<sub>2</sub> for Galactocentric annuli based on recent 21-cm and CO survey data. The synchrotron emission is computed using a parameterization of the Galactic magnetic field. Spectra of all species on the chosen grid and the  $\gamma$ -ray and synchrotron sky maps are output in standard astronomical formats for direct comparison with data, new formats in versions 54 include HEALPix<sup>3</sup> [27], and *Fermi*-LAT MapCube format for use with LAT Science Tools software<sup>4</sup>.

Also included in GALPROP are specialized routines to calculate the propagation of DM annihilation or decay products and associated diffuse  $\gamma$ -ray emission and synchrotron sky maps. The routines allow the DM profile, branching ratios, and particle spectra to be user-defined and calculate the source functions of the products of DM annihilation and  $\gamma$ -ray emissivity. The particles are then propagated as sepa-

rate species with the same propagation parameters as other CRs. The sky maps are calculated using the line-of-sight integration of the corresponding emissivities.

Details of the optimization of the code, linking to other codes (e.g., DarkSUSY [28], SuperBayeS [29, 30]) and so forth, can be found at the aforementioned website.

## 2 Diffuse Galactic and isotropic emission

The puzzling “GeV excess” relative to the predictions of diffuse  $\gamma$ -ray emission models based on locally measured CR spectra [9, 31] was an anomalous signal observed in EGRET data above  $\sim 1$  GeV. It was proposed that the GeV excess results from annihilating DM [32]. This received much attention, but a number of conventional explanations were also considered such as, e.g., variations in the CR spectra [4, 25]. Paper [33] discusses the sources of systematic uncertainties in the EGRET calibration, data handling, and in models of the diffuse emission.

Testing the origin of the GeV excess was one of the early studies of the diffuse  $\gamma$ -ray emission by the *Fermi*-LAT team [34]. The data at intermediate Galactic latitudes ( $10^\circ < |b| < 20^\circ$ ) were used in the study because the diffuse  $\gamma$ -ray emission over this region of the sky comes predominantly from relatively nearby CR nuclei interactions with interstellar gas. The *Fermi*-LAT spectrum is well reproduced by the model based on local CR measurements and inconsistent with the EGRET GeV excess. Although the *Fermi*-LAT spectral shape is consistent with the model, the overall emission in the model predictions using GALPROP was systematically low by 10-20%. This calculation employed an *a priori* model of the diffuse emission, the “conventional” model [9, 25], that is based on local CR measurements taken before the *Fermi*-LAT launch. More detailed studies of molecular clouds in the 2nd and 3rd Galactic quadrants [12, 35] show that the CR proton spectrum does not fluctuate significantly over a large Galactic volume, which supports the reasoning to use the conventional model based on local CR measurements. A comparison between the models and the *Fermi*-LAT and INTEGRAL data in the inner Galaxy is discussed in [36].

The diffuse Galactic emission presents a strong foreground signal to the much fainter diffuse extragalactic emission, which is often referred to as the extragalactic  $\gamma$ -ray background (EGB) and generally assumed to have an isotropic or nearly isotropic distribution on the sky. The EGB is composed of contributions from unresolved extragalactic sources as well as truly diffuse emission processes, such as possible signatures of large-scale structure formation, the annihilation or decay of DM, and many other processes [37].

The *Fermi*-LAT measurement of the spectrum of isotropic diffuse  $\gamma$ -ray emission from 200 MeV to 100 GeV is described in [38]. The isotropic background was found using

3. <http://healpix.jpl.nasa.gov>

4. <http://fermi.gsfc.nasa.gov/ssc/data/analysis>

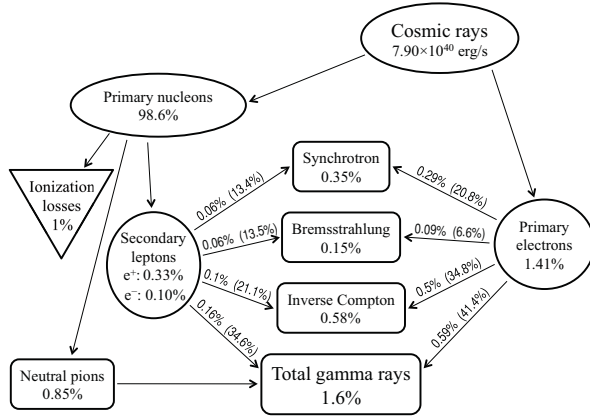


Figure 1: The luminosity budget of the Milky Way galaxy calculated for a model with 4 kpc halo [45]. The percentage figures are shown with respect to the total injected luminosity in CRs. The percentages in brackets show the values relative to the luminosity of their respective lepton populations (primary electrons, secondary electrons/positrons).

a simultaneous fit of the diffuse Galactic  $\gamma$ -ray emission as modeled using GALPROP, resolved sources from the internal *Fermi*-LAT 9-month source list (using the individual localizations but leaving the fluxes in each energy bin to be separately fitted for each source), and a model for the solar IC  $\gamma$ -ray emission [39, 40, 41]. The derived EGB spectrum is a featureless power law with index  $2.41 \pm 0.05$  and intensity  $I(> 100 \text{ MeV}) = (1.03 \pm 0.17) \times 10^{-5} \text{ cm}^{-2} \text{ s}^{-1} \text{ sr}^{-1}$ , significantly softer than the one obtained from EGRET observations [42]. Note that below 2 GeV the *Fermi*-LAT spectrum is in agreement with the spectrum found from the *reanalysis* of the EGRET data [43] which was also based on GALPROP. Using the *Fermi*-LAT-derived EGB, it was possible to set upper limits on the  $\gamma$ -ray flux from cosmological annihilation of DM [44].

### 3 Global luminosity of the Milky Way

Observations of the diffuse  $\gamma$ -ray emission from normal galaxies (LMC, SMC, M 31) and the starburst galaxies (M 82, NGC 253) by the *Fermi*-LAT [46, 47, 48, 49] and by the atmospheric Cherenkov telescopes [50, 51] show that CRs is a widespread phenomenon associated with the process of star formation. The Milky Way is the best-studied non-AGN dominated star-forming galaxy, and the only galaxy that direct measurements of CR intensities and spectra are available. However, because of our position inside, the derivation of global properties is not straightforward and requires detailed models of the spatial distribution of the emission. Meanwhile, understanding the global energy budget of processes related to the injection and propagation of CRs, and how the energy is distributed across the electromagnetic spectrum, is essential to interpret the radio/far-infrared relation [52, 53], galactic calorimetry [54], and

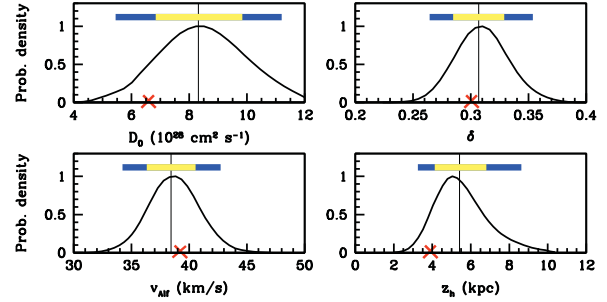


Figure 2: 1D marginalized posterior probability distribution function (PDF) normalized to the peak for the diffusion model parameters, with uniform priors assumed over the parameter ranges [58]. The cross represents the best fit, the vertical thin line the posterior mean, and the horizontal bar the 68% and 95% error ranges, respectively.

predictions of extragalactic backgrounds [55, 56, 57], and for many other studies.

Such calculations were carried out in [45]. The luminosity spectra were calculated for representative Galactic propagation models that are consistent with CR, radio, and  $\gamma$ -ray data. Figure 1 shows the detailed energy budget for a model corresponding to the middle range of the plausible models. About 1.8% of the total CR luminosity goes into the primary and secondary electrons and positrons, however, the IC scattering contributes half of the total  $\gamma$ -ray luminosity with the  $\pi^0$ -decay contributing another half. The relationship between far-infrared and radio luminosity appears to be consistent with that found for galaxies in general. The Galaxy is found to be nearly a CR electron calorimeter, but *only* if  $\gamma$ -ray emitting processes are taken into account. The synchrotron emission alone accounts for only one third of the total electron energy losses with  $\sim 10$ -20% of the total synchrotron emission from secondary CR electrons and positrons.

### 4 Constraints on CR propagation models from a global Bayesian analysis

The fully Bayesian approach to the problem of deriving constraints for CR propagation models parameters allows one to carry out a global statistical analysis of the whole parameter space, rather than be limited to scanning a reduced number of dimensions at the time. This is important in order to be able to fit simultaneously all relevant CR parameters and to explore degeneracies. While very detailed numerical models of CR propagation exist, a quantitative statistical analysis of such models has been so far hampered by the large computational effort that those models require. Although statistical analyses have been carried out before using semi-analytical models, the evaluation of the results obtained from such models is difficult, as they necessarily suffer from many simplifying assumptions.

A full Bayesian parameter estimation has been recently shown to work with a *numerical* CR propagation model [58]. Despite the heavy computational demands of a numerical propagation code, such as GALPROP, a full Bayesian analysis is possible using nested sampling and Markov Chain Monte Carlo methods (implemented in the SuperBayeS code [29, 30]). A remarkable agreement was found between the “by-eye” fitting in the past [2, 7, 11, 59] and the parameter constraints from the refined Bayesian inference analysis (Figure 2) [58]. The posterior mean values of the diffusion coefficient  $D_0 = (8.32 \pm 1.46) \times 10^{28} \text{ cm}^2 \text{ s}^{-1}$  at 4 GV and the Alfvén speed  $v_{\text{Alf}} = 38.4 \pm 2.1 \text{ km s}^{-1}$  are in fair agreement with earlier estimates of  $5.73 \times 10^{28} \text{ cm}^2 \text{ s}^{-1}$  and  $36 \text{ km s}^{-1}$  [11], respectively. The posterior mean halo size is  $5.4 \pm 1.4 \text{ kpc}$ , also in agreement with our earlier estimated range  $z_h = 4 - 6 \text{ kpc}$  [59], although our best-fit value of  $z_h = 3.9 \text{ kpc}$  is somewhat lower, due to the degeneracy between  $D_0$  and  $z_h$ . However, the well-defined posterior intervals produced in that study are significantly more valuable than just the best-fit values themselves as they provide an estimate of associated theoretical uncertainties and may point to a potential inconsistency between different types of data.

GALPROP development is supported through NASA Grants No. NNX09AC15G and NNX10AE78G.

## References

- [1] Moskalenko I. V., Strong A. W., ApJ, 1998, **493**: 694
- [2] Strong A. W., Moskalenko I. V., ApJ, 1998, **509**: 212
- [3] Vladimirov A. E. *et al.*, Computer Phys. Comm., 2011, **182**: 1156
- [4] Moskalenko I. V., Strong A. W., Reimer O., A&A, 1998, **338**: L75
- [5] Strong A. W., Moskalenko I. V., Ptuskin V. S., Ann. Rev. Nucl. Part. Sci., 2007, **57**: 285
- [6] Moskalenko I. V., Strong A. W., ApJ, 2000, **528**: 357
- [7] Moskalenko I. V. *et al.*, ApJ, 2002, **565**: 280
- [8] Moskalenko I. V. *et al.*, ApJ, 2003, **586**: 1050
- [9] Strong A. W., Moskalenko I. V., Reimer O., ApJ, 2000, **537**: 763
- [10] Strong A. W. *et al.*, A&A, 2004, **422**: L47
- [11] Ptuskin V. S. *et al.*, ApJ, 2006, **642**: 902
- [12] Abdo A. A. *et al.*, ApJ, 2010, **710**: 133
- [13] Press W. H. *et al.*, 1992, Numerical recipes in FORTRAN. The art of scientific computing, Cambridge University Press
- [14] Seo E. S., Ptuskin V. S., ApJ, 1994, **431**: 705
- [15] Mashnik S. G. *et al.*, Adv. Spa. Res., 2004, **34**: 1288
- [16] Moskalenko I. V., Mashnik S. G., Proc. 28th ICRC (Tsukuba), 2003, **4**: 1969
- [17] Webber W. R. *et al.*, ApJ Suppl., 2003, **144**: 153
- [18] Silberberg R., Tsao C. H., Barghouty A. F., ApJ, 1998, **501**: 911
- [19] Moskalenko I. V., Vladimirov A. E., Porter T. A., 2011, These Proceedings
- [20] Dermer C. D., A&A, 1986, **157**: 223
- [21] Dermer C. D., ApJ, 1986, **307**: 47
- [22] Kelner S. R., Aharonian F. A., Bugayov V. V., Phys. Rev. D, 2006, **74**: 034018
- [23] Kamae T., Abe T., Koi T., ApJ, 2005, **620**: 244
- [24] Porter T. A. *et al.*, ApJ, 2008, **682**: 400
- [25] Strong A. W., Moskalenko I. V., Reimer O., ApJ, 2004, **613**: 962
- [26] Porter T. A., Strong A., Proc. 29th ICRC (Pune), 2005, **4**: 77
- [27] Górski K. M. *et al.*, ApJ, 2005, **622**: 759
- [28] Gondolo P. *et al.*, New Astron. Rev., 2005, **49**: 149
- [29] Ruiz de Austri R., Trotta R., Roszkowski L., JHEP, 2006, **5**: 2
- [30] Trotta R. *et al.*, JHEP, 2008, **12**: 24
- [31] Hunter S. D. *et al.*, ApJ, 1997, **481**: 205
- [32] de Boer W. *et al.*, A&A, 2005, **444**: 51
- [33] Moskalenko I. V. *et al.*, Nucl. Phys. B Proc. Suppl., 2007, **173**: 44
- [34] Abdo A. A. *et al.*, Phys. Rev. Lett., 2009, **103**: 251101
- [35] Abdo A. A. *et al.*, ApJ, 2009, **703**: 1249
- [36] Strong A. W., arXiv: 1101.1381
- [37] Dermer C. D., Proc. The First GLAST Symp., ed. S. Ritz *et al.*, AIP Conf. Ser., 2007, **921**: 122
- [38] Abdo A. A. *et al.*, Phys. Rev. Lett., 2010, **104**: 101101
- [39] Moskalenko I. V., Porter T. A., Digel S. W., ApJ, 2006, **652**: L65
- [40] Orlando E., Strong A. W., Astrophys. Spa. Sci., 2007, **309**: 359
- [41] Orlando E., Strong A. W., A&A, 2008, **480**: 847
- [42] Sreekumar P. *et al.*, ApJ, 1998, **494**: 523
- [43] Strong A. W., Moskalenko I. V., Reimer O., ApJ, 2004, **613**: 956
- [44] Abdo A. A. *et al.*, JCAP, 2010, **4**: 14
- [45] Strong A. W. *et al.*, ApJ, 2010, **722**: L58
- [46] Abdo A. A. a., A&A, 2010, **512**: A7
- [47] Abdo A. A. *et al.*, A&A, 2010, **523**: A46
- [48] Abdo A. A. *et al.*, ApJ, 2010, **709**: L152
- [49] Abdo A. A. *et al.*, A&A, 2010, **523**: L2
- [50] Acciari V. A. *et al.*, Nature, 2009, **462**: 770
- [51] Acero F. *et al.*, Science, 2009, **326**: 1080
- [52] Helou G., Soifer B. T., Rowan-Robinson M., ApJ, 1985, **298**: L7
- [53] Murphy E. J. *et al.*, ApJ, 2006, **638**: 157
- [54] Voelk H. J., A&A, 1989, **218**: 67
- [55] Thompson T. A., Quataert E., Waxman E., ApJ, 2007, **654**: 219
- [56] Murphy E. J. *et al.*, ApJ, 2008, **678**: 828
- [57] Fields B. D., Pavlidou V., Prodanović T., ApJ, 2010, **722**: L199
- [58] Trotta R. *et al.*, ApJ, 2011, **729**: 106
- [59] Strong A. W., Moskalenko I. V., Adv. Spa. Res., 2001, **27**: 717